THE UNIVERSITY OF ALABAMA® | University Libraries

Fourier Analysis of Exchange Biased $Ni_{80}Fe_{20}/Fe_{50}Mn_{50}/Ni_{80}Fe_{20}$ Trilayers

G. Mankey – University of Alabama

et al.

Deposited 07/16/2019

Citation of published version:

Maat, S., et al. (1999): Fourier Analysis of Exchange Biased $Ni_{80}Fe_{20}/Fe_{50}Mn_{50}/Ni_{80}Fe_{20}$ Trilayers. *Physical Review B*, 60(14). DOI: https://doi.org/10.1103/PhysRevB.60.10252

© 1999 American Physical Society

Fourier analysis of exchange biased $Ni_{80}Fe_{20}/Fe_{50}Mn_{50}/Ni_{80}Fe_{20}$ trilayers

S. Maat, L. Shen, and G. J. Mankey
Center for Materials for Information Technology, University of Alabama, Tuscaloosa, Alabama 35487
(Received 12 March 1999; revised manuscript received 24 June 1999)

Hysteresis loops of polycrystalline and single-crystal exchange biased $Ni_{80}Fe_{20}$ (Permalloy)/$Fe_{50}Mn_{50}/Ni_{80}Fe_{20}$ (Permalloy) trilayers were measured as a function of $Fe_{50}Mn_{50}$ layer thickness with the longitudinal Kerr effect. The variation of the macroscopic pinning field H_p and the coercivity H_c was observed over a full 360° in plane rotation and Fourier analyzed. The magnetization behavior of both Permalloy layers of the polycrystalline samples was analyzed, and it was found that the pinning field of the bottom layer is always greater than for the top layer, while the situation is reversed for the coercivity due to defects incorporated in the antiferromagnetic layer. The single-crystal samples were prepared on epitaxially grown Cu(111) on Si(110), and the magnetization behavior of the top Permalloy layer was studied. In contrast to the polycrystalline samples, the coercivities peak very sharply at the easy axis, which manifests itself in large higher-order Fourier coefficients. Coercivities and loop shifts show a strong linear dependence on the antiferromagnetic layer thickness. The relation of the biasing direction to the crystal axes had no influence on H_c and H_p. This behavior is attributed to complete strain relief through the buffer layer and better crystalline growth of the trilayer as compared to the polycrystalline samples. Examination of the results with a Ginzburg-Landau energy functional verified that the Fourier coefficients obey necessary conditions to achieve energetic stability together with spontaneous magnetization. The energy functional was used to model the angular dependence of the loop shift. [S0163-1829(99)07937-0]

I. INTRODUCTION

In 1956 Meiklejohn and Bean[1] discovered that the deposition a ferromagnetic (FM) film in proximity to an antiferromagnetic (AF) film exhibits unidirectional anisotropy when cooled in a magnetic field below the Néel point of the AF film. Exchange biased thin films have found applications in magnetic thin-film sensors, such as in magnetoresistive read heads[2,3] to suppress Barkhausen noise and presently in spin-valve elements[4] for giant magnetoresonance (GMR) read heads. In spite of numerous applications, its physical origin is not understood completely yet, although considerable theoretical and experimental efforts have been made.[5] Developing an understanding of the exchange bias mechanism and the origin of the related enhancement of coercivity requires detailed measurements of multilayered systems exhibiting these effects.

Exchange bias has been studied for numerous systems, both polycrystalline and single crystal. While $Ni_{80}Fe_{20}$ is the most common FM material, many different AF materials have been employed, such as FeF_2, NiO, CoO, NiMn, IrMn, and FeMn. While the former three are insulators, the latter three are metallic antiferromagnets, which possess a finite density of states at the Fermi level. Surface states can evolve in order to match the wave functions of the delocalized electron states across the AF/FM interface. This can have a dramatic impact on the magnitude of the moments at the interface as well as the spin ordering, as opposed to insulators, which have a gap at the Fermi level. The spins are strongly coupled to the crystal lattice; therefore, crystal and interface quality plays a key role for exchange bias. In this study, a metallic single-crystal system is compared to an equivalent polycrystalline system to test the validity of the models, which are based on the assumption of localized spins. $Fe_{50}Mn_{50}$ was chosen as the antiferromagnet, since both single-crystal and polycrystalline exchange biased films can be grown.

There is strong evidence that bulk fcc γ-FeMn has a noncollinear spin structure. This has been shown experimentally[6,7] and recently in first-principles calculations.[8] Assuming naively that the spin structure is preserved at the interface, cross sections through the (111), (110), and (110) planes of $Fe_{50}Mn_{50}$ would exhibit compensated surfaces for the former two planes, but uncompensated for the latter one. Based on this assumption, a comparison of exchange biased single-crystal films with $Fe_{50}Mn_{50}$ $(hkl)/Ni_{80}Fe_{20}$ (hkl) interfaces of the three major directions showed that the (110)-oriented samples show the weakest and (111)-oriented samples the strongest loop shifts.[9,10] The (111)-oriented samples had a higher degree of chemical disorder compared to (100)- and (110)-oriented samples. A simple correlation between the strength of the biasing and the uncompensated or uncompensated nature of the surfaces was not determined. A high degree of disorder giving a high loop shift is consistent with models assuming that interfacial roughness accounts for exchange bias.[11] Difficulties in the discussion of the $Fe_{50}Mn_{50}/Ni_{80}Fe_{20}$ system may arise from the fact that it is a purely itinerant AF/FM system.

The observation of macroscopic quantities such as the loop shift H_p, also called the pinning field, and coercivity H_c can give hints as to how the spins in the AF, FM, and at their interfaces behave. Therefore we performed measurements of the angle-dependent hysteresis behavior of $Ni_{80}Fe_{20}/Fe_{50}Mn_{50}/Ni_{80}Fe_{20}$ trilayers as a function of layer thickness. A Fourier analysis of the angular-dependent Kerr data has been performed. These measurements give us the ability to model the energy surface of the system. We modeled the observed angular dependence of the pinning field within a Ginzburg-Landau model, which is very general and

 ©1999 The American Physical Society

does not depend on the material or the assumption of a particular spin structure in contrast to models based on the assumption of localized spins, which, strictly speaking, exist only in insulators. The Fourier coefficients for the pinning field are compatible with the shape of the energy surface derived from the Ginzburg-Landau model. Fourier analysis reveals differences between polycrystalline and single-crystal samples. The observed dependence of loop shifts, coercivities, and squareness of the loops on AF film thickness is consistent with assumptions of films with a constant defect density.

II. EXPERIMENT

Permalloy ($Ni_{80}Fe_{20}$)/$Fe_{50}Mn_{50}$/Permalloy ($Ni_{80}Fe_{20}$) trilayers with varying AF and FM thickness in both polycrystalline and single-crystal forms were studied. The polycrystalline trilayer samples were prepared by sputter deposition on glass substrates with an applied magnetic field of 40 Oe during deposition to impose a pinning direction upon the ferromagnetic Permalloy layers. Thickness calibration for each material was done with an atomic force microscope by scanning across an edge produced with a physical mask. First, a seed layer of 4 nm of Ta was deposited to orient the bottom Permalloy layer in the $\langle 111 \rangle$ direction.[12,13] Ta is known to promote small crystallites and smooth interfaces. The exchange properties do not depend on the thickness of the Ta layer.[13] $Fe_{50}Mn_{50}$ was grown on the bottom Permalloy layer, which grows pseudomorphic on Permalloy in the antiferromagnetic γ phase in the thickness range of our experiments.[14,15] In this phase $Fe_{50}Mn_{50}$ forms a solid solution, where Fe and Mn occupy lattice sites randomly, but their spins order antiferromagnetically. The Néel temperature of $Fe_{50}Mn_{50}$ is around 500 K so that no field cooling after deposition is necessary.[6] A second Permalloy layer was grown on top of the $Fe_{50}Mn_{50}$, and all samples were capped with 4 nm of Ta to prevent oxidation.

For comparison to the polycrystalline trilayers, single-crystal trilayers on Cu/Si(110) were investigated. Cu grows as a single crystal in the (111) orientation on Si(110).[16] A bias field parallel to the $\langle \bar{1}11 \rangle$, $\langle 1\bar{1}2 \rangle$, and $\langle 1\bar{1}0 \rangle$ directions of Si was applied to determine if interfacial strain plays a role in determining the exchange bias. The $\langle 00\bar{1} \rangle$ direction of Si coincides with the $\langle \bar{1}10 \rangle$ direction of the Cu(111) buffer, Permalloy, and $Fe_{50}Mn_{50}$, which all have the same lattice constant of $a = 3.63$ Å. The single-crystal samples were then capped with 4 nm of Cu.

All samples were characterized *ex situ*. Since the samples under investigation magnetize in plane, the longitudinal Kerr effect setup was utilized to measure their hysteresis behavior. A modulation technique proposed by Nederpel and Martens was used[17] to measure the Kerr ellipticity, which is proportional to the magnetization. The samples were mounted on a rotary table, so that it was possible to measure the coercivity and pinning field for different azimuthal angles ϕ, the angle between the applied field and the pinning direction. The hysteresis loops of the polycrystalline samples were measured from the air and glass sides of the samples. After measuring from the top, the samples were flipped over along their pinning axes and measured through the glass substrate from the bottom. Due to attenuation of the light through the $Fe_{50}Mn_{50}$, the smaller contribution in the loop could be identified with the signal from the buried Permalloy layer. For the single-crystal samples, only the hysteresis behavior of the top layer was determined.

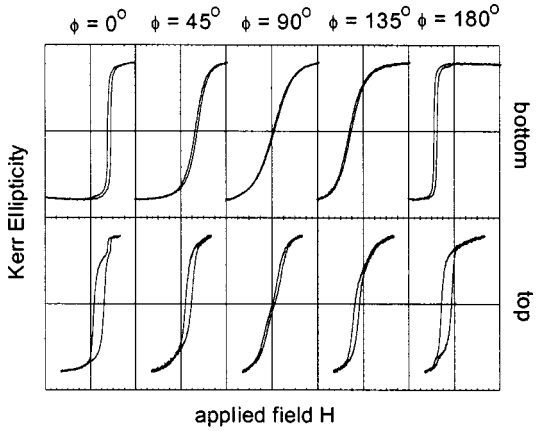

FIG. 1. Hysteresis loops of a polycrystalline exchange biased Permalloy in a Permalloy (8)/$Fe_{50}Mn_{50}$ (26)/Permalloy (4) trilayer as a function of azimuthal angle ϕ between the bias direction and the applied field during measurement. The first row shows loops measured from the bottom, the second row loops measured through the top.

Hysteresis loops measured for the polycrystalline Permalloy (8 nm)/$Fe_{50}Mn_{50}$ (26 nm)/Permalloy (4 nm) trilayer in angle increments of 45° are shown in Fig. 1. The loops acquired by measuring from the bottom are shown in the first row, while loops measured from the top are shown in the second row. Due to the attenuation of the light through the $Fe_{50}Mn_{50}$ spacer, the major contribution to the MOKE signal originates from the top Permalloy layer (T) when measured from the top side and from the bottom Permalloy layer (B) when measured from the glass side. The switching fields of the B layer observed through the bottom and top coincide. The switching of the B layer shows up in that of the T layer, but not vice versa. This is due to the fact that the bottom layer is thinner than the top layer and the MO signal scales approximately with the film thickness for thin films. The sample geometry makes it possible to identify the coercivity H_c and exchange field H_p for each Permalloy layer independently.

Both Permalloy layers are biased in the same direction. The anisotropy and exchange coupling energies of the two FM layers of the trilayers are different, and each magnetic layer switches at a different value of applied field. For an azimuthal angle of $\phi = 180°$, the loops have the same shape as the ones for $\phi = 0°$ under the symmetry operation $\mathbf{H} \rightarrow -\mathbf{H}$ and $\mathbf{M} \rightarrow -\mathbf{M}$. The coercivity H_c and pinning field H_p have been measured as functions of the azimuthal angle ϕ between the pinning direction (at $\phi = 0°$) and applied field. Some basic properties of these quantities can be derived from some simple symmetry arguments.[18] H_p and H_c trivially must possess the symmetry of a full rotation and therefore must have the symmetry properties $H_P(\phi) = H_P(\phi + 2\pi)$ and $H_c(\phi) = H_c(\phi + 2\pi)$. When each spin in the multilayer is rotated in the plane by π and the field is applied in the opposite direction, the same hysteresis behavior with $H \rightarrow -H$ and $M \rightarrow -M$ must be observed. So the pinning

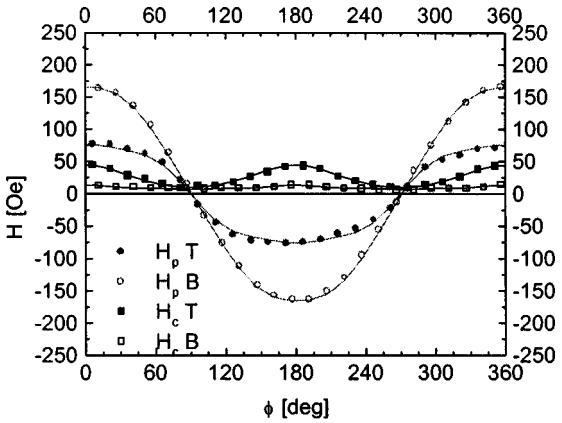

FIG. 2. Angular dependence of coercivity H_c and pinning field H_p for the top and bottom Permalloy layers of the polycrystalline Permalloy (8)/$Fe_{50}Mn_{50}$ (26)/Permalloy (4) sample.

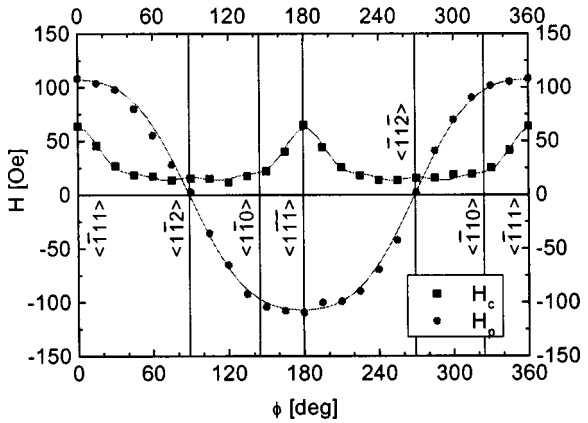

FIG. 3. Angular dependence of coercivity H_c and pinning field H_p for the top Permalloy layer of the single-crystal Si(110)/Cu(111)/Permalloy (8)/$Fe_{50}Mn_{50}$ (32)/Permalloy (4) trilayer, biased parallel to the $\langle 1\bar{1}1\rangle$ direction of the Si.

field must have the symmetry $H_P(\phi)=-H_P(\phi+\pi)$ and the coercivity the symmetry $H_C(\phi)=H_C(\phi+\pi)$; i.e., H_c is π periodic and H_p a 2π periodic function. Hence H_c can be expanded in even cosine terms and H_p in odd cosine terms. This is not sufficient to prove that H_c and H_p have the same phase. However, if we deal only with a single unidirectional anisotropy, so that $H_c(\phi)=H_c(-\phi)$ and $H_p(\phi)=H_p(-\phi)$, it is reasonable to assume that the phase is fixed to zero. The foregoing arguments are independent of the mechanism producing the exchange bias.

The angle-dependent data for the coercivity H_c and the pinning field H_p for a polycrystalline $Ni_{80}Fe_{20}$ (8 nm)/$Fe_{50}Mn_{50}$ (28 nm)/$Ni_{80}Fe_{20}$ (4 nm) sample are shown in Fig. 2. The pinning field between $0°<\phi<90°$ and $270°<\phi<360°$ is positive and between $90°<\phi<270°$ is negative. The sign of H_p should not be confused with negative and positive exchange biases. It merely originates from applying the external field in opposite directions. All measured samples showed a negative exchange bias, i.e., a loop shift in the opposite direction of the field applied during deposition. The coercivity shows pronounced maxima at $\phi=0°$ and $\phi=180°$ with a smaller half width than the minima, at $\phi=90°$ and $\phi=270°$, which coincide with the zeros of H_p. This is similar to what was observed for exchange biased polycrystalline Permalloy on CoO.[18,19]

The angular dependence of H_c and H_p for the top Permalloy layer of a single-crystalline $Ni_{80}Fe_{20}$ (8)/$Fe_{50}Mn_{50}$ (32)/$Ni_{80}Fe_{20}$ (4) trilayer biased parallel to the $\langle 1\bar{1}1\rangle$ direction of Si is shown in Fig. 3. Their coercivities peak very sharply at the easy axes in contrast to the more gradual change around the easy axes in the polycrystalline samples, which can be associated with the distribution of crystallites resulting in a distribution of easy directions. Samples with 24- and 32-nm-thick $Fe_{50}Mn_{50}$ layers were studied.

No differences in the behavior and magnitude of H_c and H_p were found for samples biased along the different crystallographic directions, and the maximum pinning field and coercivity always occur along the bias axis. These data show that the Cu buffer layer of 100 nm is thick enough to relieve the in-plane strain, such that no in-plane dependence on the biasing direction of H_c and H_p can be observed. The measurements also show that the contribution of the crystalline anisotropy to the angular dependence of the exchange bias behavior is negligible. This is distinct from FeF_2, where the biasing of an Fe overlayer parallel and perpendicular to the [001] and $[1\bar{1}0]$ directions of the uncompensated (110) FeF_2 surface yielded dramatically different results.[20–22] This can be explained by the lower crystalline anisotropy of $Fe_{50}Mn_{50}$ compared to FeF_2.

III. FOURIER ANALYSIS

A Fourier series with even terms was used to fit the experimental results for H_c,

$$H_c=H_c^0(1+f_1^c\cos 2\phi+f_2^c\cos 4\phi+\cdots) \tag{1}$$

and a Fourier series with odd terms was used to fit those for H_p,

$$H_p=H_p^0(\cos\phi+f_1^p\cos 3\phi+f_2^p\cos 5\phi+\cdots). \tag{2}$$

Equation (2) shows the unidirectional nature of the pinning field. No more than three Fourier terms were used to obtain a numerical error lower than 1% for every Fourier component in the case of the polycrystalline samples. The coefficients f_3 in both series (1) and (2) are already so small that they have the same order of magnitude as the numerical error of the fit. The single-crystal results required only two Fourier coefficients to fit H_p, but five to fit H_c, to obtain a similar numerical error.

The coercivity H_c and pinning field H_p of the T and B layers of the polycrystalline sample for different $Fe_{50}Mn_{50}$ spacers for the easy directions ($\phi=0°$) are plotted in Fig. 4(a). The coercivity of the bottom layer is smaller than that of the top layer for all thicknesses measured. For the pinning field the situation is reversed. The pinning field of the bottom layer stays well above the pinning field of the top layer. The pinning field H_p and coercivity H_c decrease linearly with $Fe_{50}Mn_{50}$ thickness for both layers. The slope of the lines for H_p for the B and T layers is approximately the same and H_c of the T layer is decreasing faster than for the B layer. H_p and H_c for the single crystal are plotted in Fig. 4(b). Both quantities decrease for the thicker sample and were not influenced by the biasing direction.

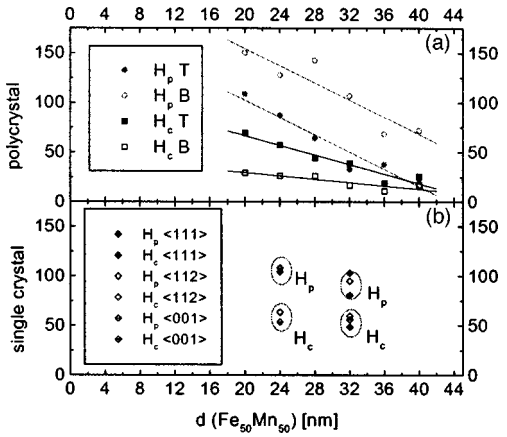

FIG. 4. Thickness dependence of coercivity and pinning field for the easy axis for (a) polycrystalline and (b) single-crystal Permalloy (8)/$Fe_{50}Mn_{50}$ (X)/Permalloy (4) trilayers.

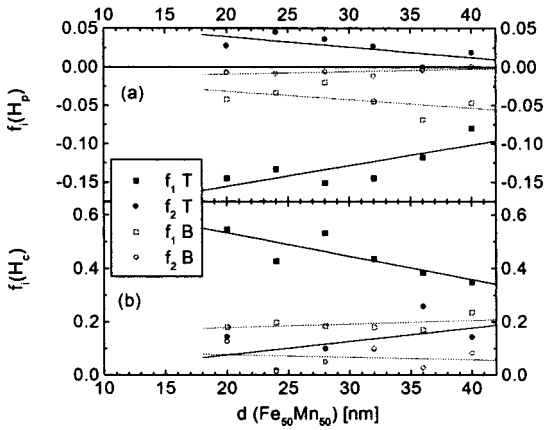

FIG. 6. Fourier components of H_c (top) and H_p (bottom) vs $Fe_{50}Mn_{50}$ thickness d for top and bottom Permalloy layers of the polycrystalline samples.

The observation that the order in which $Fe_{50}Mn_{50}$ and Permalloy are grown has an influence on the magnitude of H_c and H_p is in agreement with earlier work on the same trilayer system[14] as well as for CoO/Permalloy bilayers.[23] However, we measure a decreasing pinning field for the B layer with increasing $Fe_{50}Mn_{50}$ thickness as opposed to a constant pinning field for the B layer for a system with thick Permalloy layers ($B=60$ nm, $T=20$ nm).

Coercivity is a measure of defects incorporated at the interface. The fact that the coercivity of the top layer is higher than that of the bottom layer indicates that more defects are at the top $Fe_{50}Mn_{50}$/Permalloy interface. The squareness of a loop, i.e., the ratio of remnant to saturation moment, gives a hint of the angular spread of an easy axis. For an exchange biased sample, the remnant moment is defined for $H_{\mathrm{appl}}=H_p$ rather than for $H_{\mathrm{appl}}=0$. Figure 5 shows the squareness for bottom and top Permalloy layers. The T layers show a smaller squareness than the B layers, indicating that the angular spread of their easy directions is higher than for the bottom layer. This observation also implies that more defects are at the top AF/FM interface.

The Fourier coefficients for H_p and H_c of the polycrystalline $Ni_{80}Fe_{20}$ (8 nm)/$Fe_{50}Mn_{50}$ (X nm)/$Ni_{80}Fe_{20}$ (4 nm) films are plotted in Figs. 6(a) and 6(b), respectively. The Fourier coefficients f_1^p for both T and B layers in the Fourier series of H_p are negative and increase towards zero with increasing $Fe_{50}Mn_{50}$ thickness for all samples analyzed. Measurements on polycrystalline Permalloy/CoO systems show a dip in the azimuthal curve along the easy direction, which also indicates a large negative f_1^p component.[18,19] Here f_2^p is negative for the B layers and positive for the T layers. The Fourier coefficients for H_c are all positive.

For the single-crystal trilayers, the higher-order Fourier coefficients for H_c are all positive, but larger than for the polycrystalline samples, which shows up in the angular plot in Fig. 3 as sharp peaks at the easy axis. The top row of Fig. 7 shows the Fourier coefficient f_1^p, the second the coefficients $f_1^c-f_4^c$. As opposed to the polycrystalline samples, f_2^p was negligible. All coefficients for the coercivity are positive and show a decreasing tendency with AF layer thickness. The biasing directions with respect to the Si(110) substrate are indicated in the three columns.

The signs of the Fourier coefficients for H_p can be explained using a Ginzburg-Landau energy functional,[24] which we restrict to the fifth power in m in the assumption that our observations can be modeled within this approximation:

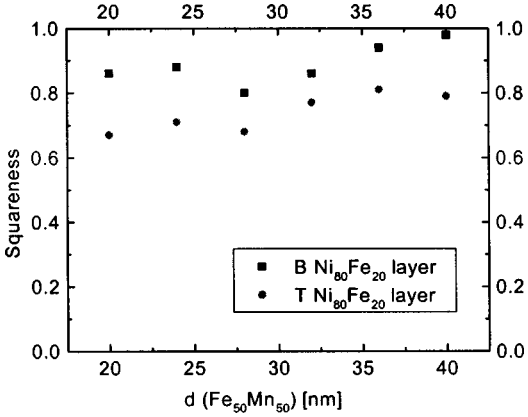

FIG. 5. Squareness of the hysteresis loops measured of top and bottom Permalloy layers of the polycrystalline samples.

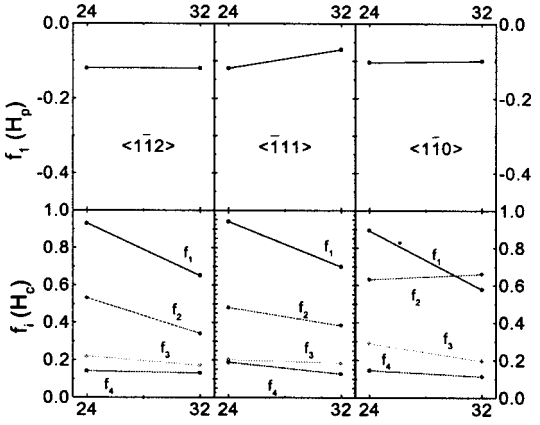

FIG. 7. Fourier components of H_p and H_c of the top Permalloy layer vs thickness d of $Fe_{50}Mn_{50}$ of the single-crystal trilayers. The top row shows the coefficient f_1^p of the pinning field, the bottom row the coefficients $f_1^c-f_4^c$ of the coercivity. The biasing directions in reference to the Si substrate are indicated in the columns.

$$F(m(\phi))=am+\frac{1}{2}bm^2+\frac{1}{3}cm^3+\frac{1}{4}dm^4+\frac{1}{5}em^5 +\cdots-hm, \tag{3}$$

where $m(\phi)=\cos\phi$ is the normalized magnetization. We will relate this functional to our data and show that in order to achieve energetic stability together with spontaneous magnetization in an exchange-biased sample, f_1^p must be of negative sign. f_2^p, however, can be of either sign. The last term in the functional is the Zeeman energy, and for an ordinary ferromagnet the coefficients *a*, *c*, and *e*, i.e., the coefficients for the odd terms in *F*, are necessarily zero because of symmetry upon time reversal. In the case of an exchange biased ferromagnet, this argument does not hold. The deposition of the ferromagnet in the vicinity of an antiferromagnet creates a domain wall in the antiferromagnet,[25] which introduces a loop shift in the hysteresis of the ferromagnet and breaks time inversion symmetry. If a sufficiently high field is applied along one of the directions of the easy axis, the magnetization switches completely in the direction of the applied field. Therefore minima of *F* exist for $m=1$ and $m=-1$ and the necessary condition

$$\frac{\partial F}{\partial m}=a+bm+cm^2+dm^3+em^4\Big|_{m=1}^{m=-1}=0 \tag{4}$$

must be fulfilled.

From Eq. (4) we can derive the following two equations:

$$b+d=0 \tag{5a}$$

and

$$a+c+e=0. \tag{5b}$$

Equation (5a) is the usual one found for an unbiased ferromagnet within the Ginzburg-Landau approach. For stability it is necessary for *b* and *d* to be nonzero. These terms are responsible for the creation of a double well, which causes irreversible switching and coercivity. Assuming a gradually decrease of Fourier coefficients, it can be inferred from Eq. (5b) that *e* is a small quantity compared to *a* and *c*, and thus *a* and *c* will necessarily be of opposite signs.

Further, the conditions for minima at $m=1$ and $m=-1$ are

$$\frac{\partial^2 F}{\partial m^2}(+1)>0 \tag{6a}$$

and

$$\frac{\partial^2 F}{\partial m^2}(-1)>0, \tag{6b}$$

from which we derive the two inequalities

$$-b+c+2e>0 \tag{7a}$$

and

$$-b-c-2e>0. \tag{7b}$$

The combination of Eqs. (7a) and (7b) yields

$$-b-c>2e>-b+c. \tag{8}$$

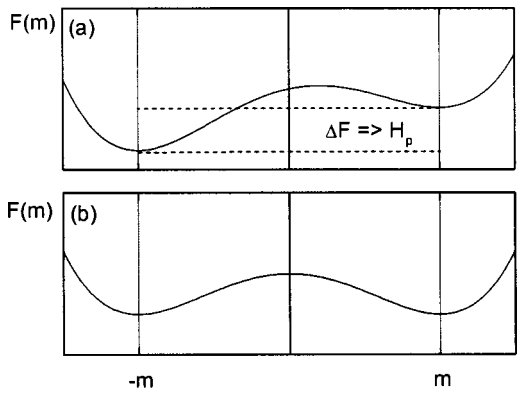

FIG. 8. Cross section through the energy surface for $m_y=0$ for (a) a biased and (b) an unbiased ferromagnet.

Figure 8(a) represents the cross section through the energy surface of an exchange biased ferromagnet at $m_y=0$ without an applied field and Fourier coefficients according to the foregoing discussion:

$$F(\phi)=\frac{1}{5}\cos\phi-\frac{1}{2}\cos^2\phi-\frac{1}{15}\cos^3\phi+\frac{1}{4}\cos^4\phi. \tag{9}$$

Figure 8(b) represents the same for an equivalent unbiased sample with $b=-1$ and $d=1$. The loop shift of H_p is determined between the difference of the energy of $F(1)$ and $F(-1)$ of opposite directions as indicated in Fig. 8(a):

$$\begin{aligned} H_p(\phi)&\propto F(\phi)-F(\phi-\pi)\\ &=2\left(am+\frac{1}{3}cm^3+\frac{1}{5}em^5\right)\\ &=\left(2a+\frac{1}{2}c+\frac{1}{4}e\right)\cos\phi+\left(\frac{1}{6}c+\frac{1}{8}e\right)\cos 3\phi\\ &\quad+\frac{1}{40}e\cos 5\phi=\left(\frac{7}{4}a+\frac{1}{4}c\right)\cos\phi\\ &\quad+\left(-\frac{1}{8}a+\frac{1}{24}c\right)\cos 3\phi+\left(-\frac{1}{40}a-\frac{1}{40}c\right)\cos 5\phi\\ &=H_p^0(\cos\phi+f_1^p\cos 3\phi+f_2^p\cos 5\phi), \end{aligned} \tag{10}$$

where the relations

$$\cos^3 x=\frac{1}{4}(\cos 3x+3\cos x), \tag{11a}$$

$$\cos^5 x=\frac{1}{16}(\cos 5x+5\cos 3x+10\cos x) \tag{11b}$$

have been used.

From Eq. (10), it can be seen that f_1^p is must be negative, since *a* and *c* are of approximately the same order of magnitude if *e* is small and f_2^p can be of either positive or negative sign, in agreement with our measurements. Simulations for $e=0$ and $e=-\frac{1}{40}$ are shown in Figs. 9(a) and 9(b), respectively. The first function fits our results very well. The second one, although *e* is small, is distinct from the former one. It possesses relative extrema for $\phi=0°$ and $\phi=180°$

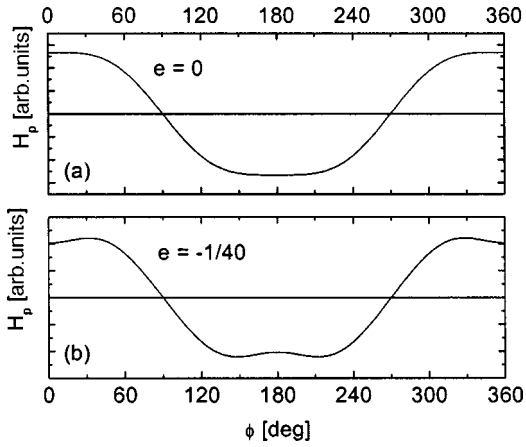

FIG. 9. Simulation of the dependence of the macroscopic pinning field H_p on the azimuthal angle ϕ. The first case (a) with $e=0$ resembles the measurements for the $Fe_{50}Mn_{50}/Ni_{80}Fe_{20}$ system (compare to Fig. 2), while the second one (b) with $e=-1/40$ resembles the $CoO/Ni_{80}Fe_{20}$ bilayer system (Refs. 18 and 19).

and resembles the observations of the Permalloy/CoO bilayer system,[18,19] where the pinning field had shown these relative extrema along the easy axis, indicating that higher-order odd cosine terms are necessary to fit the results.

The coefficients $a-e$ are temperature dependent: b becomes positive above the Curie point, and a, c, and e are zero above the blocking temperature where the loop shift vanishes. However, each coefficient may have a different temperature characteristic, causing the angular dependence of the loop shift to become strongly temperature dependent when the blocking temperature is approached.

Recently, the traditional method to identify the loop shift with the exchange energy was put under debate.[26,27] For a real sample the energy surface will vary from location to location, since defects such as dislocations and stacking faults are incorporated in a film. Magnetization reversal along an easy direction or axis is normally associated with nucleation of magnetic domains. The nucleation will take place first at the smallest energy barrier of the two minima and the loop shift measured along an easy axis will be determined by the energy surface at this location. If only reversible changes close to the easy axis are considered, the energy required to cant all moments by the same angle, then the exchange field is determined by the overall average shape of the surface energy. Our complete analysis probes the entire energy surface and gives indications of the importance of defect concentrations in the trilayers.

IV. SUMMARY

Exchange biased $Ni_{80}Fe_{20}/Fe_{50}Mn_{50}/Ni_{80}Fe_{20}$ trilayers were investigated by magneto-optical Kerr measurements. The pinning field and coercivity was measured over a 360° in-plane rotation and their curves fitted to Fourier series of odd and even trigonometric terms, respectively, which have been justified by symmetry arguments independent of the exchange mechanism between AF and FM layers. The Fourier components for H_p and H_c were analyzed for their dependence on the $Fe_{50}Mn_{50}$ thickness. It was shown experimentally that the second-order Fourier coefficient for H_p is of different sign from the first one. The third one was negative for the bottom and positive for the top Permalloy layers in the polycrystalline samples and negligible in the single-crystal samples.

The higher-order Fourier coefficients of H_c of the single-crystal samples are generally much larger than those for the polycrystalline samples. This manifests itself in a sharply peaked coercivity at the easy axis. A sharply peaked coercivity was also observed in polycrystalline exchange-coupled $Ni_{81}Fe_{19}$ (25 nm)/$Cr_{45.5}Mn_{45.5}Pt_9$ (60 nm), although no AF thickness dependence on the behavior was reported.[28] These quantities exhibit a strong dependence on the AF thickness for both single-crystal and polycrystalline samples. Further, for the single-crystal samples, the biasing direction relative to the crystal axes had no influence on H_p and H_c. Examination within a Ginzburg-Landau energy functional under the inclusion of odd terms due to violation of time-inversion symmetry verified that the different signs of the leading coefficients are necessary to achieve, energetically, stability together with spontaneous magnetization. The angular dependence of the loop shifts was simulated within the model. Accumulating defects are held responsible for the thickness dependence of the loop shift and coercivity. Future work will include a Fourier analysis of H_c and H_p in dependence on the FM layer thickness and temperature. The angular dependence of both quantities should change significantly when the blocking temperature is approached.[28]

ACKNOWLEDGMENTS

This work was supported by Army Research Office Grant No. DAAH 04-96-1-0316 and shared equipment through NSF MRSEC Grant No. DMR-9809423.

[1] W. H. Meiklejohn and C. P. Bean, Phys. Rev. **102**, 1413 (1956); **105**, 904 (1957).
[2] C. Tsang, R. E. Fontana, T. Lin, and D. E. Heim, IEEE Trans. Magn. **30**, 3801 (1994).
[3] C. Tsang, IEEE Trans. Magn. **25**, 3692 (1989).
[4] B. Dieny, V. S. Speriosu, S. S. P. Parkin, B. A. Gurney, D. R. Wilhoit, and D. Mauri, Phys. Rev. B **43**, 1297 (1991).
[5] J. Nogués and I. K. Schuller, J. Magn. Magn. Mater. **192**, 203 (1999).
[6] H. Umebayashi and Y. Ishikawa, J. Phys. Soc. Jpn. **41**, 1195 (1976).
[7] S. J. Kennedy and T. J. Hicks, J. Phys. F **17**, 1599 (1987).
[8] T. C. Schulthess, W. H. Butler, G. M. Stocks, S. Maat, and G. J. Mankey, J. Appl. Phys. **85**, 4842 (1999).
[9] R. Jungbluth, R. Coehoorn, M. T. Johnson, J. aan de Stegge, and A. Reinders, J. Appl. Phys. **75**, 6659 (1994).
[10] R. Jungbluth, R. Coehoorn, M. T. Johnson, C. Sauer, P. J. van der Zaag, A. R. Ball, T. G. S. M. Rijks, J. aan der Stegge, and A.

Reinders, J. Magn. Magn. Mater. **148**, 300 (1995).
[11] A. P. Malozemoff, Phys. Rev. B **35**, 3679 (1987); **37**, 7673 (1988); J. Appl. Phys. **63**, 3874 (1988).
[12] R. Jerome, T. Valet, and P. Galtier, IEEE Trans. Magn. **30**, 4878 (1994).
[13] A. Choukh, IEEE Trans. Magn. **33**, 3676 (1997).
[14] K. T. Y. Kung, L. K. Louie, and G. L. Gorman, J. Appl. Phys. **69**, 5634 (1991).
[15] C. Hwang, R. H. Geiss, and J. K. Howard, J. Appl. Phys. **64**, 6115 (1988).
[16] H. Jiang, T. J. Klemmer, J. A. Barnard, and E. A. Payzant, J. Vac. Sci. Technol. A **16**, 3376 (1998).
[17] P. Q. J. Nederpel and J. W. D. Martens, Rev. Sci. Instrum. **56**, 687 (1985).
[18] T. Ambrose, R. L. Sommer, and C. L. Chien, Phys. Rev. B **56**, 83 (1997).
[19] N. J. Gökemeijer, T. Ambrose, and C. L. Chien, Phys. Rev. Lett. **79**, 4270 (1997).
[20] J. Nogués, D. Lederman, T. J. Moran, and I. K. Schuller, Appl. Phys. Lett. **68**, 3186 (1996).
[21] J. Nogués, D. Lederman, T. J. Moran, and I. K. Schuller, Phys. Rev. Lett. **76**, 4624 (1996).
[22] T. J. Moran, J. Nogués, D. Lederman, and I. K. Schuller, Appl. Phys. Lett. **72**, 617 (1998).
[23] T. Ambrose, K. Leifer, K. J. Hemker, and C. L. Chien, J. Appl. Phys. **81**, 5007 (1997).
[24] K. Huang, *Statistical Mechanics*, 2nd ed. (Wiley, New York, 1987).
[25] D. Mauri, H. C. Siegmann, P. S. Bagus, and E. Kay, J. Appl. Phys. **62**, 3047 (1987).
[26] B. H. Miller and E. D. Dahlberg, J. Appl. Phys. **81**, 5002 (1997).
[27] E. D. Dahlberg, B. H. Miller, B. Hill, B. J. Johnson, V. Strom, K. V. Rao, J. Nogués, and I. K. Schuller, J. Appl. Phys. **83**, 6893 (1998).
[28] H. Xi, M. H. Kryder, and R. M. White, Appl. Phys. Lett. **74**, 2687 (1999).